CrystEngComm

www.rsc.org/crystengcomm

Volume 15 | Number 24 | 28 June 2013 | Pages 4787–4982

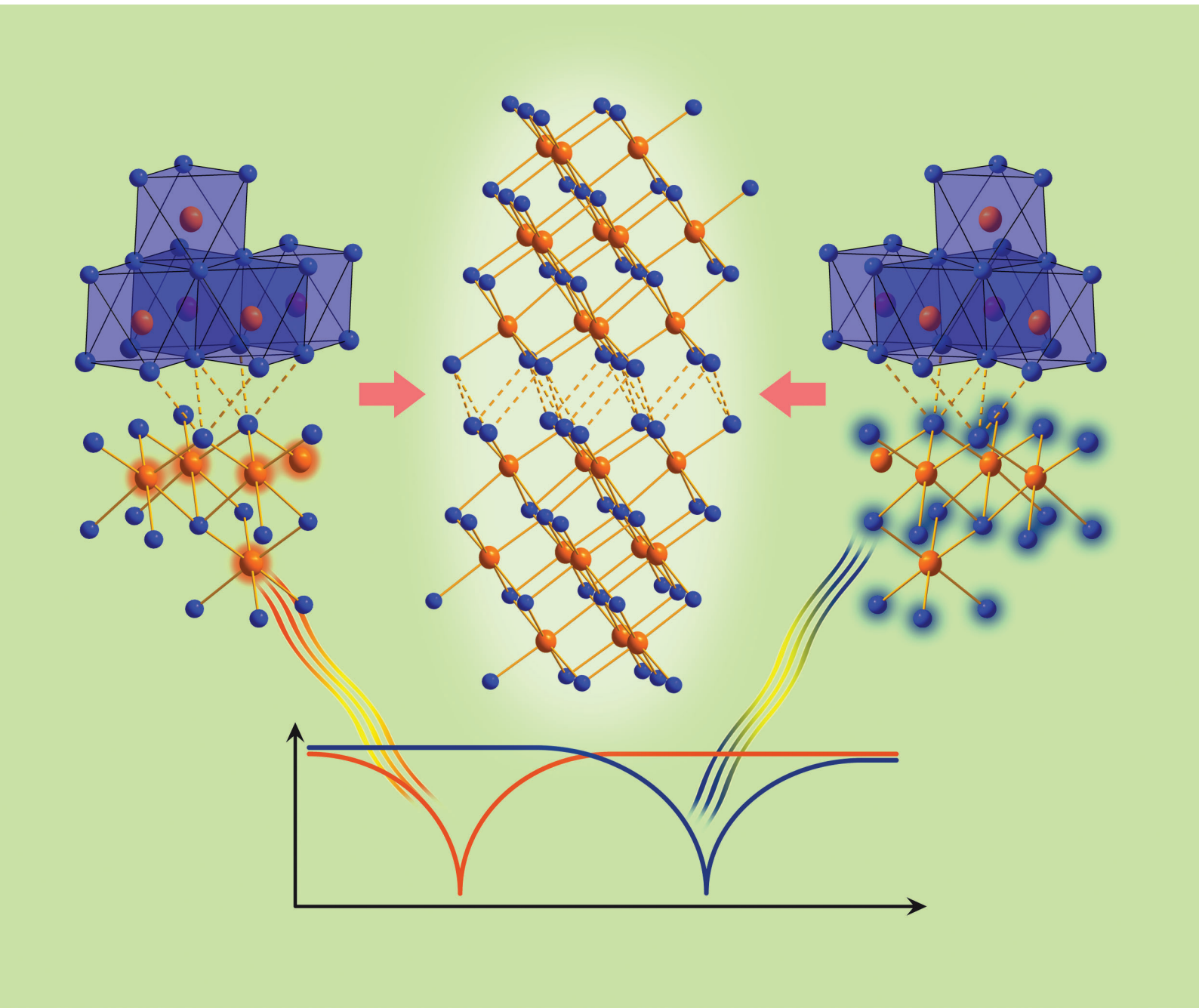

RSC Publishing

COVER ARTICLE

Oeckler *et al.*

Temperature dependent resonant X-ray diffraction of single-crystalline $Ge_2Sb_2Te_5$

CrystEngComm

RSC Publishing

PAPER

View Article Online
View Journal | View Issue

Temperature dependent resonant X-ray diffraction of single-crystalline $Ge_2Sb_2Te_5$†

Cite this: *CrystEngComm*, 2013, **15**, 4823

Philipp Urban,[a] Matthias N. Schneider,[b] Loredana Erra,[c] Simon Welzmiller,[a] Felix Fahrnbauer[a] and Oliver Oeckler*[ab]

The element distribution in the crystal structure of the stable phase of the well-known phase-change material $Ge_2Sb_2Te_5$ was determined at temperatures up to 471 °C using single crystals synthesized by chemical transport reactions. Because of the similar electron count of Sb and Te, the scattering contrast was enhanced by resonant diffraction using synchrotron radiation (beamline ID11, ESRF). A simultaneous refinement on data measured at the *K*-absorption edges of Sb and Te as well as at additional wavelengths off the absorption edges yielded reliable occupancy factors of each element on each position (a = 4.2257(2) Å, c = 17.2809(18) Å, $P\bar{3}m1$, R_1 (overall) = 0.037). The dispersion correction terms $\Delta f'$ were refined and match experimental ones obtained from fluorescence spectra by the Kramers–Kronig transform. The structure contains distorted rocksalt-type blocks of nine alternating cation and anion layers, respectively, which are separated by van der Waals gaps between Te atom layers. Ge atoms prefer the cation positions near the center of the rocksalt-type block (occupancy factors $Ge_{0.60(4)}Sb_{0.36(2)}$), Sb atoms the one near the van der Waals gap ($Ge_{0.33(7)}Sb_{0.66(4)}$). Anti-site disorder is not significant. During heating up to 471 °C and subsequent cooling, a reversible structural distortion was observed. The refinements show that with increasing temperature the first pair of anion and cation layers next to the van der Waals gap becomes slightly detached from the block and increasingly resembles a GeTe-type layer. Thus, the difference between interatomic distances in the 3 + 3 cation coordination sphere of the mixed Ge–Sb position next to the gap becomes more pronounced. The element distribution, in contrast, neither changes during the heating experiment nor upon long-time annealing. Thus, the behavior of 9P-$Ge_2Sb_2Te_5$ single crystals is predominantly under thermodynamic control.

Received 3rd December 2012,
Accepted 14th January 2013

DOI: 10.1039/c3ce26956f

www.rsc.org/crystengcomm

Introduction

Germanium antimony tellurides (GST materials) are widely used as phase-change materials (PCMs) in devices for optical data storage like DVD-RAM or Blu-Ray disks as well as for the electrical write–read–erase processes in non-volatile RAM.[1–3] Materials with the same chemical compositions also exhibit interesting thermoelectric properties.[4,5]

In phase-change devices, GST materials are applied as thin films. The phase change between a metastable crystalline phase and an amorphous one can be induced by thermal or electrical energy. In rewritable optical storage media, a laser beam supplies different short-time thermal treatments for switching between the two states. The reading process relies on the different optical or electrical contrast between them.

$Ge_2Sb_2Te_5$, which is used in DVD-RAM devices,[6] probably represents the most well-known PCM and has been discussed in many publications, both concerning its actual applications as well as more fundamental aspects, because it is an ideal model system for PCMs in general.[7] The metastable crystalline phase exhibits a rocksalt-type average structure with Ge, Sb and vacancies on the cation and tellurium on the anion position.[8] This phase has not yet been obtained as a compact bulk material and also does not correspond to a high-temperature phase, in contrast to materials with higher GeTe contents $(GeTe)_nSb_2Te_3$ ($n \geqslant 3$).[5,9] Bulk material of $Ge_2Sb_2Te_5$ usually contains the stable modification that does not exhibit cation vacancies. It exhibits a trigonal layered structure with a 9P-type stacking sequence $[A{=}C{-}A{-}C{-}A{-}C{-}A{-}C{=}A]_\infty$ of anion (A) and cation (C) layers.[10,11] These form distorted rocksalt-type slabs separated by van der Waals gaps (*cf.* Fig. 3). The bonds (=) between the Te atoms and the cations next to the van der Waals gap are shorter than the bonds in the center of the block, which can be explained by the low coordination number of the Te atoms next to the gap.

As the structure of the distorted rocksalt-type slabs can be viewed as a model system for the local bonding situation in the

[a]*IMKM, Leipzig University, Scharnhorststr. 20, 04275 Leipzig, Germany. E-mail: oliver.oeckler@gmx.de; Fax: +49 (0)341-9736299; Tel: +49 (0)341-9736251*
[b]*Department of Chemistry, LMU Munich, Butenandtstr. 5-13 (D), 81377 Munich, Germany*
[c]*ESRF, Polygone Scientifique Louis Néel, Grenoble, 38000, France*

† Electronic supplementary information (ESI) available. CSD 425044–425053. See DOI: 10.1039/c3ce26956f

disordered metastable phase of PCMs, it is an intriguing task to analyze it in detail and to study its changes at various temperatures, especially as it has been shown that diffusion phenomena play a crucial role in GST materials above 300 °C.[12] This is also reflected in the discontinuous behavior of their thermoelectric properties at this temperature as shown for $(GeTe)_n(Sb_2Te_3)$ (n = 3–19).[5]

So far, high-quality single crystals have not been described in the literature and structure analyses using powder data[10] have limited accuracy concerning the atom distribution on all positions due to the lacking scattering contrast of Sb and Te, which have very similar electron counts. In order to reliably and independently determine the exact distribution of the elements on the cation positions and to address the question if there is a significant amount of anti-site defects, conventional (laboratory) X-ray diffraction is not sufficient. X-ray diffraction with monochromatic synchrotron radiation is a powerful tool to distinguish between these elements even when they share one position if the effect of anomalous dispersion is exploited. In order to benefit from this effect, datasets have to be collected near the absorption edges of the respective elements. Then, the atomic form factor $f(\lambda,\theta) = f^0(\sin\theta/\lambda) + \Delta f'(\lambda) + i\Delta f''(\lambda)$ (dependent on the diffraction angle θ and the wavelength λ) is characterized by very significant dispersion correction terms $\Delta f'$ and $\Delta f''$, which are small when a wavelength that is far off an absorption edge is used. The scattering contrast between Sb and Te can be increased by up to 8 electrons per element for which such resonant absorption-edge data are present.[13]

In this contribution we present the first single-crystal study on $Ge_2Sb_2Te_5$, which allows us to discuss structural details at various temperatures.

Experimental

Sample preparation and characterization

Single crystals of $Ge_2Sb_2Te_5$ were prepared by chemical vapor transport. A stoichiometric mixture of Ge (Aldrich, 99.999%), Sb (Smart Elements, 99.9999%) and Te (Alfa Aesar, 99.999%) was sealed in a silica glass ampoule under dry argon and heated to 950 °C for 2 h. After quenching in water, the product was crushed and 20 wt% SbI_3 were added as transport agent (total weight: 140 mg). The mixture was sealed in a silica glass ampoule (length: ~20 cm; diameter: 15 mm) under vacuum and placed in a two-zone furnace. Chemical transport took place from 585 °C to 525 °C for 17.5 hours. Single crystals of up to 0.2 mm in size were obtained. After washing with acetone in order to remove traces of the transport agent, the crystals were sealed in silica glass capillaries under dry argon. The composition of the crystal used for the diffraction experiments (*cf.* Fig. 1) was determined after the investigation by EDX analysis using a JSM-6500F scanning electron microscope (Jeol, USA) equipped with an EDX detector (model 7418, Oxford Instruments, Great Britain). The resulting composition $Ge_{28(3)}Sb_{22(1)}Te_{50(2)}$ (averaged from 10 measuring points) is in agreement with the nominal composition $Ge_2Sb_2Te_5$ = $Ge_{22}Sb_{22}Te_{56}$ within the error limits of the method. Analyses on other crystals from the same sample yielded similar results.

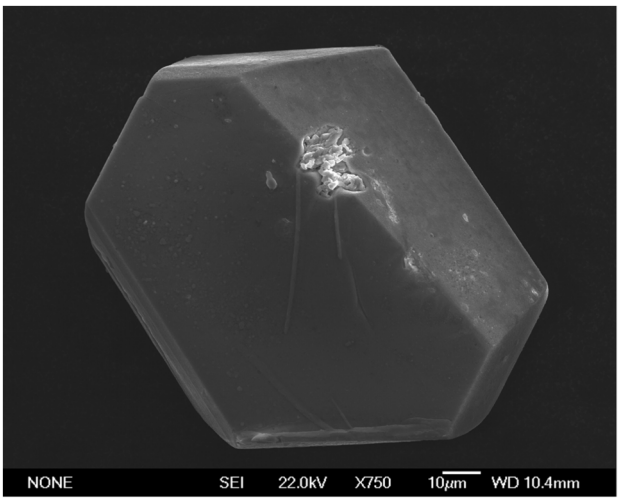

Fig. 1 SEM image of the single crystal investigated (the small damage results from the removal of the crystal from the capillary after the measurement).

Single crystal X-ray diffraction

Single crystal X-ray diffraction was performed on a heavy-duty diffractometer (Huber, Germany) at the Materials Science Beamline ID11[14] (ESRF, Grenoble, France) with tunable wavelength. Intensities were measured using a FReLoN2K CCD detector (dynamical range 2^{16}).[15] Additional high-angle data were collected employing a detector offset. For heating experiments, a gas blower GSB 1300 (ESRF, Grenoble, France) controlled by an Eurotherm controller (Eurotherm/Invensys, Great Britain) was installed at the beamline. The temperature was calibrated by melting and recrystallizing samples of Bi, Te and KI (melting points 271.3 °C, 450 °C and 681 °C, respectively). Fluorescence spectra were measured with an X-flash detector (Rontec, Germany). Additional diffraction experiments were performed on an IPDS-I diffractometer (Stoe & Cie., Germany) with Ag Kα radiation (0.56087 Å). For the accurate determination of the lattice parameters, X-ray powder diffraction data of a stoichiometric bulk sample of $Ge_2Sb_2Te_5$ were obtained on a HUBER G670 diffractometer with Cu Kα1 radiation (Ge(111)-monochromator, 1.54051 Å) and a Stadi-P diffractometer equipped with a graphite furnace (Mo Kα1 radiation, Ge(111)-monochromator, 0.70926 Å).

Synchrotron diffraction data were indexed with SMART[16] and integrated with SAINT.[17] Semiempirical absorption correction, as well as scaling and merging the different datasets for each wavelength was performed with SADABS[18] taking into account the Laue symmetry $\bar{3}m$. Laboratory single-crystal diffraction data were processed with the diffractometer software[19] and XPREP.[20] The final structure refinements were performed with JANA2006,[21] additional test refinements were also done with SHELX-97.[22] Dispersion correction terms $\Delta f'$ and $\Delta f''$ for the different wavelengths were taken from the NIST database,[23] $\Delta f'$ values were refined using JANA2006 for the elements at the respective edges. Fluorescence data were

transformed to $\Delta f'$ and $\Delta f''$ values with CHOOCH.[24] Powder data were evaluated with WinXPOW;[25] lattice parameters were determined by Rietveld refinements with TOPAS.[26]

Results and discussion

Element distribution in the as-synthesized crystal at ambient temperature

Synchrotron datasets of the $Ge_2Sb_2Te_5$ single crystal were measured on the low-energy side of the *K*-absorption edges of Sb (0.40681 Å; 30.477 keV), Te (0.38979 Å; 31.808 keV) and at a wavelength far off the edges (0.56356 Å; 22.000 keV). A measurement exactly at the absorption edge was avoided due to the pronounced slope of $\Delta f''$ at that energy and the uncertainty involved; the low-energy side is favorable due to lower absorption. The dispersion correction terms derived from the experimental fluorescence data are displayed in Fig. 2. A comparison between experimental, database and refined values is given in Table 1.

The refined values match both the experimental ones and those from the database quite well, which indicates that the chemical environment of the corresponding atoms has no pronounced influence in this case. In the final refinement, the dispersion correction terms with the highest influence, *i.e.* $\Delta f'$ of the elements at their absorption edges, were refined. The *R* values improved more than one would expect just from 2 additional parameters. All dispersion correction terms used are summarized in Table 2. These values were also used for the refinements of the high-temperature data (see below).

Table 1 Dispersion correction term $\Delta f'$ near the absorption edges of Sb and Te from fluorescence data, the NIST-database (interpolated) and the refined values

Edge	λ/Å	$\Delta f'$/e (exp.)	$\Delta f'$/e (NIST)	$\Delta f'$/e (refined)
Sb	0.40681	−5.86	−5.68	−6.38(36)
Te	0.38979	−6.02	−5.62	−6.72(7)

In the initial steps of the structure refinement, the site occupancies for Ge, Sb and Te were refined independently on all positions. The ones that were zero within their standard deviations were set to zero in subsequent refinements. The anion positions turned out to be occupied exclusively by Te, which means that there is no significant anti-site disorder. The results of the structure refinement are listed in Tables 3 and 4. Both Ge and Sb atoms occupy the two cation positions. Ge atoms prefer the site GeSb2 (2d), Sb the site GeSb4 (2c) next to the van der Waals gap. The reason for this unbalanced site occupancy is probably the higher oxidation state of Sb^{III} compared to Ge^{II}. This leads to a more favorable charge balance in the coordination sphere of Te5, which is only coordinated by 3 cations. Te1, in contrast, is octahedrally coordinated and Te3, as well as all the cations, exhibits a 3 + 3 coordination. The structure is depicted in Fig. 3. The model basically corresponds to that mentioned in the literature;[10] however, this is the first structure refinement of $Ge_2Sb_2Te_5$ with no constrained composition or site occupancies. In addition, the precision of the interatomic distances is approximately ten times higher and the displacement parameters could be refined anisotropically.

Bond valence calculations using VaList[27] support the unbalanced cation distribution. The calculated bond valence sum for Ge is 1.773 for the position Ge2 and 1.653 for Ge4, so a concentration of germanium on the position Ge2 in the center of the block is reasonable, compared to the theoretical

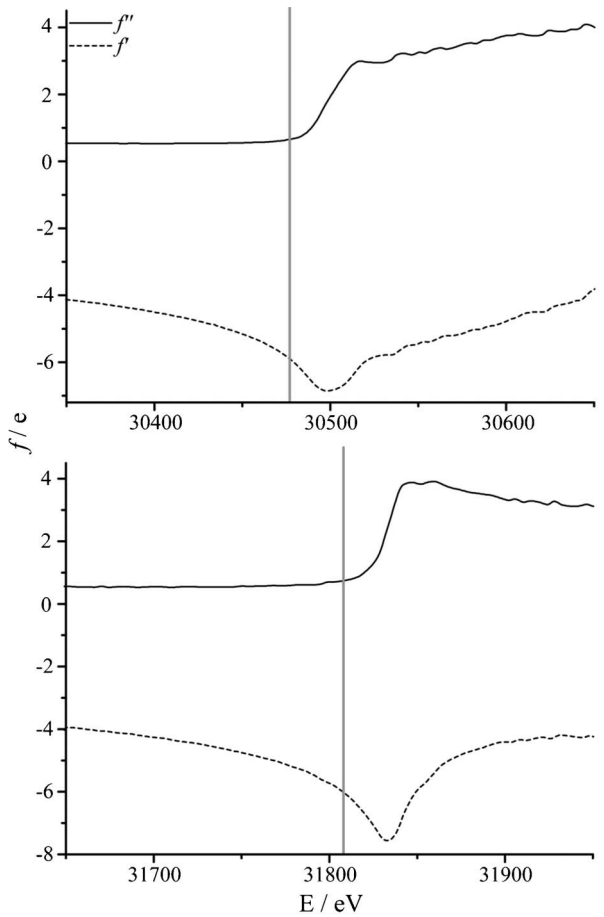

Fig. 2 Dispersion correction terms $\Delta f'$ and $\Delta f''$ calculated from fluorescence data; top: around the Sb edge, bottom: around the Te edge. The energy where diffraction data were acquired is marked by vertical lines.

Table 2 Dispersion correction terms used for the final structure refinement from the NIST database or refined values (with standard deviations)

λ/Å	Element	$\Delta f'$/e	$\Delta f''$/e
0.56356	Ge	0.40	1.18
	Sb	−0.71	1.02
	Te	−0.61	1.11
0.40681	Ge	0.38	0.64
	Sb	−6.38(36)	0.64
	Te	−2.33	0.61
0.38979	Ge	0.38	0.64
	Sb	−2.03	3.36
	Te	−6.72(7)	0.73

Table 3 Crystal data and results of the structure refinement at room temperature

Refined composition	$Ge_{1.9(2)}Sb_{2.0(1)}Te_5$		
Molecular weight (g mol^{-1})	1022.4		
Temperature (K)	293		
Lattice parameters[i] (Å)	a = 4.2257(2), c = 17.2809(18)		
Cell volume (Å^3)	267.24(3)		
Crystal system	Trigonal		
Space group	$P\bar{3}m1$		
$\rho_{calc.}$ (g cm^{-3})	6.35		
Z	1		
F(000)	424		
Beamline	ID11 (ESRF, Grenoble)		
Radiation	Synchrotron		
λ (Å)	0.56356	0.40681	0.38979
Energy (keV)	22.000	30.477	31.808
Reflections (independent)	3348 (371)	5112 (553)	9227 (553)
R_{int} (obs/all)	0.0377/0.0380	0.0494/0.0510	0.0492/0.0506
μ (mm^{-1})	12.5	7.8	18.2
sinθ/λ (Å^{-1})	0.57	0.79	0.83
Absorption correction	Semiempirical[18]		
Parameters	23 (6 constraints)[ii]		
Weighting scheme	w = $1/[\sigma^2(F_o) + 0.000225(F_o^2)]$		
R_1 [$I > 3\sigma(I)$]	0.0272	0.0325	0.0225
wR [$I > 3\sigma(I)$]	0.0344	0.0446	0.0288
R_1 (all)	0.0380	0.0352	0.0282
wR (all)	0.0359	0.0362	0.0291
	For all data in all datasets		
R_1 [$I > 3\sigma(I)$]	0.0275		
wR [$I > 3\sigma(I)$]	0.0324		
R_1 (all)	0.0371		
wR (all)	0.0334		
Goof (all)	1.28		
$\Delta\rho_{min}/\Delta\rho_{max}$ (e Å^{-3})	−1.5/+3.6 (averaged)		

[i]From powder data [ii]Ge2/Sb2 and Ge4/Sb4, respectively, were refined with equal coordinates and displacement parameters.

oxidation state of +2. For Sb, the calculated values are 3.216 for Sb2 and 2.997 for Sb4. So an enrichment of Sb near the van der Waals gap on position Sb4 is favorable if the theoretical oxidation state of +3 is assumed. Te5 has a bond valence sum of 1.735, which is not far from the theoretical value of −2. So this irregular cation distribution stabilizes the 3 fold coordinated Te5 next to the van der Waals gap. An ordered arrangement with Ge exclusively on position GeSb2 would lead to a low bond valence for Te1.

Changes in the crystal structure at elevated temperatures

High-temperature diffraction datasets were collected *in situ* at 213 °C, 316 °C, 419 °C and 471 °C during heating and cooling the crystal. As the crystal cannot be kept at the same temperature when the wavelength is changed (its position in the beam would need to be realigned), only one dataset per temperature could be measured. It was collected near the absorption edge of Sb (0.40681 Å) to enhance at least part of the scattering contrast. Additional laboratory X-ray diffraction data (IPDS-I, Ag Kα) were collected *ex situ* after the high temperature measurements and after annealing the crystal for two weeks at 471 °C. As the composition does not change upon heating, it was constrained according to $Ge_2Sb_2Te_5$ in all these refinements. Then, electroneutrality in the 9P-type structure requires that every Wyckoff site is fully occupied. Anti-site defects were neglected as test refinements indicated that they were not significant within a 3σ range, therefore, all three Te positions can be assumed to be fully occupied and only one parameter, *i.e.* the occupancy of Ge2, which equals that of Sb4, is sufficient to describe all site occupancies. This yields a very stable refinement. The refined dispersion correction term for

Table 4 Coordinates, equivalent isotropic and anisotropic displacement parameters and site occupancies of $Ge_2Sb_2Te_5$ at room temperature (U_{eq} = 1/3[U_{33} + 4/3(U_{11} + U_{22} − U_{12})]; U_{13} = U_{23} = 0; U/Å^2)

Atom	Wyckoff position	x	y	z	U_{eq}	$U_{11} = U_{22} = 2U_{12}$	U_{33}	sof
Te1	1a	0	0	0	0.01696(11)	0.01707(13)	0.01673(19)	1
Ge2 Sb2	2d	2/3	1/3	0.10635(2)	0.02783(15)	0.02564(19)	0.0322(3)	0.60(4) 0.36(2)
Te3	2d	1/3	2/3	0.204549(16)	0.01733(9)	0.01768(11)	0.01662(14)	1
Ge4 Sb4	2c	0	0	0.32532(2)	0.02581(14)	0.02331(17)	0.0308(2)	0.33(7) 0.66(4)
Te5	2d	2/3	1/3	0.418105(18)	0.02085(10)	0.02094(12)	0.01047(6)	1

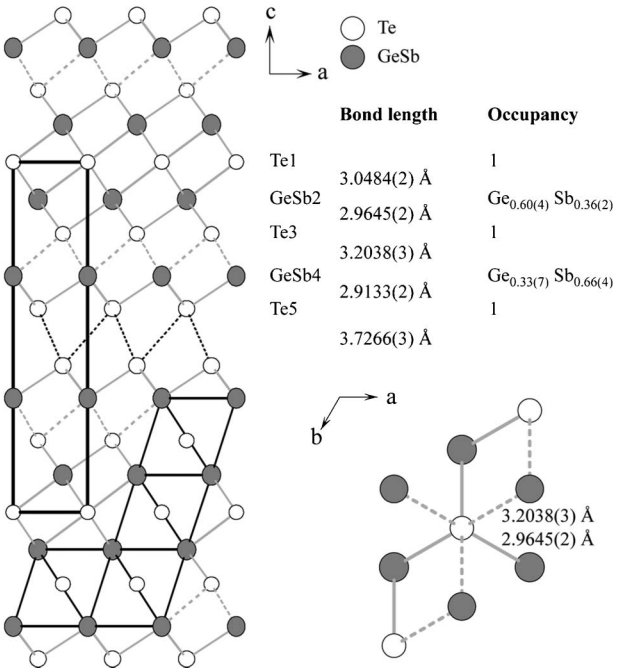

Fig. 3 Crystal structure of $Ge_2Sb_2Te_5$ (left): longer bonds are drawn with gray broken lines, Te–Te contacts across the van der Waals gap are drawn as dotted black lines; one unit cell is outlined. The pseudooctahedral coordination of Te is shown in the lower right part of the drawing, displacement ellipsoids of all atoms are drawn with 93% probability. Top right: bond lengths and site occupancies; bottom right: 3 + 3 coordination of Te3.

Sb from the joint room-temperature calculation was used and not further refined, so that the site occupancies appear with smaller standard deviations compared with the room temperature structure refinement; however, this is just a consequence of the suppressed correlation between the occupancies and the dispersion correction terms and of the parameter coupling. Some representative structure parameters and quality criteria are summarized in Tables 5 and 6, respectively.

The atom distribution does not change significantly during heating, cooling and annealing the crystal, as also mentioned before.[10] This indicates that the element distribution is thermodynamically stable over the whole temperature range. The quality criteria remained in the same range for all refinements except the one of the annealed crystal. Concerning the interatomic distances, there are significant reversible changes with temperature. The Te–Te distance at the van der Waals gap and also the distance between Te3 and GeSb4 (*cf.* Fig. 3) increase when the crystal is heated and decrease in the same manner when it is cooled (*cf.* Fig. 4 bottom). The pseudooctahedral 3 + 3 coordination spheres around GeSb2, Te3 and GeSb4 become more distorted when the crystal is heated. The most significant changes occur in the vicinity of the van der Waals gap. The deviation from undistorted octahedral coordination around GeSb4 is the most pronounced change at high temperature. The ratio long bond/short bond, which is a measure for the deviation from a regular octahedron, increases to 1.106. The atoms GeSb4 and Te5, thus, almost form a layer (Ge/Sb)–Te. When heated, this

Table 5 Selected results of the structure refinements of $Ge_2Sb_2Te_5$ at different temperatures (↑ heating, ↓ cooling)

Temp.	Data	sof (Sb4)	*z* (Sb4)	*z* (Te5)	V^a/Å^3
RT	3 datasets	0.66(4)	0.32532(2)	0.418107(18)	267.24(4)
RT	Sb-edge	0.683(10)	0.32531(5)	0.41807(3)	267.24(4)
213 °C ↑	Sb-edge	0.663(11)	0.32565(6)	0.41794(4)	269.73(4)
316 °C ↑	Sb-edge	0.667(10)	0.32572(6)	0.41776(4)	271.16(5)
419 °C ↑	Sb-edge	0.651(11)	0.32577(7)	0.41760(5)	271.83(8)
471 °C	Sb-edge	0.647(11)	0.32579(8)	0.41744(5)	272.40(7)
419 °C ↓	Sb-edge	0.659(11)	0.32566(8)	0.41755(5)	271.83(8)
316 °C ↓	Sb-edge	0.644(14)	0.32546(7)	0.41760(5)	271.16(5)
213 °C ↓	Sb-edge	0.671(12)	0.32538(7)	0.41775(5)	269.73(4)
RT	Ag Kα	0.619(14)	0.32524(6)	0.41799(4)	267.24(4)
Annealed	Ag Kα	0.61(2)	0.32531(12)	0.41815(8)	267.24(4)

[a] From powder data.

approximately GeTe-type layer is increasingly detached from the remaining NaCl-type block. The bond length to Te3 increases, as the van der Waals gap does. In the center of the block the changes are less pronounced but also significant. The structure tends to be more layer-like at higher temperatures. There is no trend towards a cubic structure with randomly ordered vacancies.

In contrast to all compounds with $(GeTe)_n(Sb_2Te_3)$ with $n > 2$, there is no cubic high-temperature phase. The reason could be the unfavorably low coordination of many atoms in a hypothetical NaCl-type $Ge_2Sb_2Te_5$ due to the very high vacancy concentration of 20%. The layered structure is thermodynamically stable up to the melting point. The metric distortion of the structure at elevated temperatures is pronounced; however, although the cations are probably mobile,[12] diffusion processes do not lead to a different overall cation distribution or reconstructive structural changes.

Conclusions

Three conclusions can be drawn from the results of the structure refinements.

1. The Te position next to the van der Waals gap has a low coordination number. Therefore, Sb atoms prefer the positions next to these Te atoms, because this way the local charge balance is better saturated. This leads to the formation of a GeTe-type layer, which increasingly detaches from the rocksalt-type block at increasing temperature.

2. The behavior of the structure during heating is probably comparable with that of metastable crystalline phases in thin films of phase-change materials. Locally, in such compounds, there may be pronounced deviations from an ideal rocksalt-type structure.[28] The thermodynamic stability of layered structures and distorted coordination octahedra may lead to short-range order, especially in compounds such as $Ge_2Sb_2Te_5$ itself, due to the extraordinarily high vacancy concentration in a metastable rocksalt-type phase.

3. In crystalline long-range ordered germanium antimony tellurides, kinetic effects do not play a significant role, in contrast to their huge impact in metastable quenched

Table 6 Quality criteria of the refinements of the structure of $Ge_2Sb_2Te_5$ at elevated temperatures

Temp.	Data	R_1 (obs)	R_1 (all)	wR (obs)	wR (all)	Goof (all)	Refl.	obs.	$\Delta\rho_{min/max}$
RT	3 datasets	0.027	0.037	0.032	0.033	1.28	553	390	−1.50/3.60
RT	Sb-edge	0.028	0.038	0.033	0.034	1.33	460	346	−3.35/6.45
213 °C ↑	Sb-edge	0.030	0.045	0.035	0.036	1.31	461	312	−1.21/4.10
316 °C ↑	Sb-edge	0.029	0.049	0.032	0.034	1.16	465	284	−1.41/3.30
419 °C ↑	Sb-edge	0.031	0.058	0.035	0.037	1.21	462	266	−0.89/2.89
471 °C	Sb-edge	0.035	0.062	0.037	0.040	1.31	464	253	−0.96/3.12
419 °C ↓	Sb-edge	0.035	0.058	0.037	0.039	1.32	460	275	−1.48/3.62
316 °C ↓	Sb-edge	0.036	0.057	0.038	0.040	1.37	466	286	−1.21/4.46
213 °C ↓	Sb-edge	0.039	0.057	0.040	0.042	1.50	467	311	−1.84/5.83
RT	Ag Kα	0.035	0.056	0.040	0.042	1.63	634	427	−1.85/3.14
Annealed[a]	Ag Kα	0.048	0.056	0.071	0.083	1.18	319	259	−1.80/2.30

[a] During annealing, the crystal quality decreased; therefore a higher instability factor in the weighting scheme was required to keep the refinement stable; thus, the corresponding quality criteria are not fully comparable to the ones resulting from the earlier measurements.

phases.[12] The cation disorder is not a consequence of limited diffusion as it changes neither at high temperatures nor during annealing.

Acknowledgements

The authors thank Christian Minke (LMU Munich) for SEM operation and EDX analyses, Thomas Miller (LMU Munich) for the temperature-dependent powder diffraction experiments, Gavin Vaughan and Jonathan Wright (ESRF) for discussing experimental details of the synchrotron measurements and maintaining the beamline. Furthermore, we are indebted to Prof. Dr. W. Schnick (LMU Munich) for his generous support of this work.

This investigation was funded by the Deutsche Forschungsgemeinschaft (grant OE530/1-2).

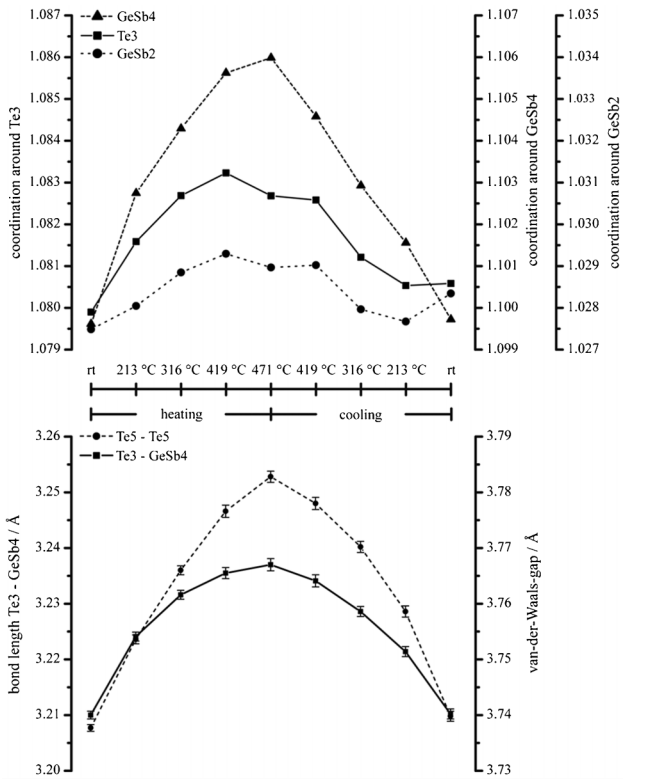

Fig. 4 Changes in the crystal structure of $Ge_2Sb_2Te_5$ at elevated temperatures; top: 3 + 3 coordination (ratio of the longer/shorter interatomic distance from the central atom to the vertices of the distorted coordination octahedron, *cf.* Fig. 3 bottom right); bottom: temperature dependence of selected interatomic distances (*cf.* text).

References

1 M. Wuttig and N. Yamada, *Nat. Mater.*, 2007, **6**, 824.
2 S. Raoux, *Annu. Rev. Mater. Res.*, 2009, **39**, 25.
3 V. Giraud, J. Cluzel, V. Sousa, A. Jacquot, A. Dauscher, B. Lenoir, H. Scherrer and S. Romer, *J. Appl. Phys.*, 2005, **98**, 013520.
4 M. N. Schneider, T. Rosenthal, C. Stiewe and O. Oeckler, *Z. Kristallogr.*, 2010, **225**, 463.
5 T. Rosenthal, M. N. Schneider, C. Stiewe, M. Döblinger and O. Oeckler, *Chem. Mater.*, 2011, **23**, 4349.
6 I. Satoh and N. Yamada, *Proc. SPIE–Int. Soc. Opt. Eng.*, 2001, **4085**, 283.
7 J. Hegedüs and S. R. Elliott, *Nat. Mater.*, 2008, **7**, 399.
8 N. Yamada and T. Matsunaga, *J. Appl. Phys.*, 2000, **88**, 7020.
9 M. N. Schneider, P. Urban, A. Leineweber, M. Döblinger and O. Oeckler, *Phys. Rev. B: Condens. Matter Mater. Phys.*, 2010, **81**, 184102.
10 T. Matsunaga, N. Yamada and Y. Kubota, *Acta Crystallogr., Sect. B: Struct. Sci.*, 2004, **60**, 685.
11 O. G. Karpinsky, L. E. Shelimova, M. A. Kretova and J.-P. Fleurial, *J. Alloys Compd.*, 1998, **268**, 112.
12 M. N. Schneider, X. Biquard, C. Stiewe, T. Schröder, P. Urban and O. Oeckler, *Chem. Commun.*, 2012, **48**, 2192.
13 A. K. Cheetham and A. P. Wilkinson, *Angew. Chem., Int. Ed. Engl.*, 1992, **31**, 1557.
14 G. B. M. Vaughan, J. P. Wright, A. Bytchkov, C. Curfs, C. Grundlach, M. Orlova, L. Erra, H. Gleyzolle, T. Buslaps, A. Götz, G. Suchet, S. Petitdemange, M. Rossat, L. Margulies, W. Ludwig, A. Snigirey, I. Snigireva, H. O. Sørensen, E. M. Lauridsen, U. L. Olsen, J. Oddershede and H. F. Poulsen, *Challenges Mater. Sci. Possibilities 3D 4D*

Charact. Tech., Proc. Risoe Int. Symp. Mater. Sci., 31st, 2010, **521**, 457.
15 J.-C. Labiche, O. Mathon, S. Pascarelli, M. A. Newton, G. G. Ferre, C. Curfs, G. Vaughan, A. Homs and D. F. Carreiras, *Rev. Sci. Instrum.*, 2007, **78**, 091301.
16 J. L. Chambers, K. L. Smith, M. R. Pressprich and Z. Jin, *SMART*, V5.059, Bruker AXS, Madison, USA, 1997–98.
17 *SAINT*, V6.36A, Bruker AXS, Madison, USA, 1997–2002.
18 *SADABS*, V2.05, Bruker AXS, Madison, USA, 1999.
19 Stoe & Cie GmbH, Darmstadt, Germany, 1997–99.
20 *XPREP*, V6.12, Bruker AXS, Madison, USA, 2001.
21 V. Petricek, M. Dusek and L. Palatinus, *JANA2006 – The Crystallographic Computing System*, Institute of Physics, Praha, Czech Republic, 2006.
22 G. M. Sheldrick, *Acta Crystallogr., Sect. A: Found. Crystallogr.*, 2008, **64**, 112.
23 C. T. Chantler, K. Olsen, R. A. Dragoset, J. Chang, A. R. Kishore, S. A. Kotochigova and D. S. Zucker, *X-Ray Form Factor, Attenuation and Scattering Tables*, Version 2.1, National Institute of Standards and Technology, Gaithersburg, MD, 2005.
24 G. Evans and R. F. Pettifer, *J. Appl. Crystallogr.*, 2001, **34**, 82.
25 *WINXPOW*, V2.12, Stoe & Cie GmbH, Darmstadt, Germany, 2005.
26 A. Coelho, *TOPAS – Academic*, V4.1, Coelho Software, Brisbane, 2007.
27 A. S. Wills, *VaList*, Program available from www.ccp14.ac.uk.
28 M. Wuttig, D. Lüsebrink, D. Wamwangi, W. Wełnic, M. Gilleßen and R. Dronskowski, *Nat. Mater.*, 2007, **6**, 122.